ELSEVIER

Spatial variability of atrazine sorption parameters and other soil properties in a podzoluvisol

Diederik Jacques [a,*], Christophe Mouvet [b], Binayak Mohanty [c], Harry Vereecken [d], Jan Feyen [a]

[a] *Institute for Land and Water Management, Katholieke Universiteit Leuven, Vital Decosterstraat 102, B-3000 Leuven, Belgium*
[b] *BRGM, Department of Hydrology, Geochemistry and Transfers, BP 6009, avenue Claude Guillemin, 45060 Orléans cédex 2, France*
[c] *U.S. Salinity Laboratory, USDA-ARS, 450 West Big Springs Road, Riverside, CA 92507, USA*
[d] *Forschungszentrum Jülich, Institut für Chemie und Dynamik der Geosphäre IV, DE-52425, Jülich, Germany*

Abstract

The spatial variability of the K_f and n parameters of the Freundlich sorption isotherm for atrazine and their correlation with soil textural variables, cation exchange capacity and organic carbon content were studied in a stagnic podzoluvisol. Ninety-three sample points were organized on an irregular three-dimensional grid to a depth of 3.2 m. A trend in the vertical direction explains, for most variables, about 85% of the observed variance. This trend also significantly influences the observed correlation structure between the variables. The horizontal and vertical trends were removed from the data set with the median polish algorithm. The residuals resulting from this technique obey the intrinsic hypothesis. Organic carbon content, cation exchange capacity and n revealed spatial structure. The estimated correlation length scales in the vertical direction were between 0.63–0.81 m for n and the organic carbon content, and between 0.25–0.40 m for the cation exchange capacity. The variograms of sand, loam, clay and K_f exhibited pure nugget. The correlation structures between the variables differ for different spatial increments. Variables appeared correlated at small spatial increments whereas they are not correlated if the spatial location of the sample points is neglected. © 1999 Elsevier Science B.V. All rights reserved.

Keywords: Multivariate geostatistics; Hydrology; Stochastic processes; Transport; Sorption; Median polish

* Corresponding author. Tel.: + 32-16-32-97-21; fax: + 32-16-32-97-60; e-mail: diederik.jacques@agr.kuleuven.ac.be

1. Introduction

A recent review of pesticide transport through field soils (Flury, 1996) showed experimental evidence supporting the occurrence of pesticide leaching to groundwater in sandy, loamy and clayey soils. Furthermore, Flury (1996) stressed the importance of preferential flow phenomena for the leaching of very strongly adsorbing pesticides (e.g., Kladivko et al., 1991; Flury et al., 1995; Traub-Eberhard et al., 1995). Field experiments contribute significantly to the understanding of transport of adsorbable and degradable solutes and reveal problems related to pesticide transport at field-scale. In addition, controlled laboratory experiments may provide experimental evidence for different physical and chemical processes in the soil system such as pesticide adsorption at multiple sites with different kinetic adsorption–desorption rates or with irreversible reactions such as hydrolysis (e.g., Brusseau et al., 1989; Ma and Selim, 1994). Analytical or numerical models may be alternatives to investigate the effects of different processes on pesticide transport. Such tools can be used to evaluate the effect of different assumptions on pesticide breakthrough curves or to quantify the relative importance of certain local-scale transport processes on field-scale transport in physically and chemically heterogeneous soils. The present study provides relevant data on the spatial variability of nonlinear adsorption parameters of atrazine which may be used in various modelling studies.

Numerical studies have shown that the dispersion of a solute plume moving downwards in a soil is significantly influenced by the spatial variability of the soil hydraulic properties (Tseng and Jury, 1994; Roth and Hammel, 1996; Vanderborght et al., 1997). Besides physical heterogeneity, chemical heterogeneity of the soil has also a major impact on the longitudinal dispersion of reactive solutes as was shown in the studies of Jury and Gruber (1989) and van der Zee and Boesten (1991). The effect of both physical and chemical heterogeneities on pesticide movement in the unsaturated zone for linearly adsorbing pesticides was recently investigated by Yang et al. (1996a,b). They assumed either a perfectly positive or negative correlation, or no correlation, between the saturated hydraulic conductivity, K_s, and the adsorption coefficient, K_d. Both the analytical (Yang et al., 1996a) and the numerical (Yang et al., 1996b) analyses indicate that pesticide spreading is larger if K_s and K_d are negatively correlated in comparison with the positively correlated or the uncorrelated case, and that dispersion is enhanced with larger geometric means of the adsorption coefficient. Bellin and Rinaldo (1995) found that the dispersion of the pesticide plume is also affected by the degree of correlation between the physical and chemical properties for pesticide transport under saturated conditions.

Although the variability of pesticide sorption parameters significantly influences the transport of pesticides through the unsaturated and saturated zones, and although a positive, a negative, or no correlation between K_d and K_s is assumed in many modelling and theoretical studies, little information is available about the variability and the spatial correlation structure of the sorption parameters and their correlation with other soil parameters. Recently, Beck et al. (1996) investigated the spatial and temporal variability of the adsorption and desorption coefficient of isoproturon in a cultivated structured clay soil. The present paper analyzes the spatial structure of atrazine sorption

parameters and soil properties from an experimental site near Jülich, Germany (Vereecken et al., 1996).

The main objective of this work was to study the spatial variability of the parameters of the Freundlich isotherm for atrazine (AT: 2-chloro-4-ethylamino-6-isopropylamino-1,3,5-triazine) sorption in the vadose zone and to quantify different factors contributing to the observed spatial variability. A second objective of this study was to explore the consistency of the spatial correlation between the different soil properties at different spatial scales.

2. Materials and methods

2.1. Experimental design

Percent sand, loam, and clay, organic carbon content (OC), cation exchange capacity (CEC) and atrazine (AT) sorption parameters (K_f and n), measured on soil samples to a depth of 3.2 m, were taken from an extended data set (Vereecken et al., 1996). Samples were taken from the Krauthausen experimental site near Jülich, Germany. This site was under meadow for several years. The soil is classified as a stagnic podzoluvisol (FAO, Driessen and Dudal, 1991) and has five distinct horizons: Ap horizon (0–30 cm), eluvial Eg horizon (30–40 cm), Btg1 horizon (40–60 cm), gleyic Btg2-horizon (60–100 cm), and a C2 horizon (> 100 cm). The general soil texture at the experimental site is loamy with clay percentages ranging between 20 and 30%. A specific geological profile of the site was established on the basis of four boreholes to the depths of 15 and 20 m (two boreholes per depth) (Vereecken et al., 1996). These boreholes revealed a 20-cm thick stony layer at a depth between 1.0 to 1.3 m below surface. Below the stony layer, between 1.3 and 4.0 m, there was a layer of dark-brown gravel deposited by the Rur which was poorly sorted compared to the underlying Rhine sediments between 4.0 and 11.0 m depth.

In total, 93 soil samples were collected at several depths in and around three boreholes, the coordinates of which, in a local reference system, are (-33.83 m, 58.6 m) for borehole 7, (-9.7 m, 21.44 m) for borehole 22, and (-29.18 m, 32.44 m) for borehole 32. The boreholes were chosen in such a way that they were independent from each other and matched the groundwater sampling protocol (Vereecken et al., 1996). In borehole 7, 11 samples were taken to a depth of 1.25 m with a vertical increment of 0.1 m; four additional samples were taken between 1.25 m and 2.65 m depth. In the other two boreholes, nine samples were taken to a depth of 3.1 m, with a vertical increment of 0.2 m in the top 1 m and approximately 0.4 m increment in the subsoil. Soil samples were also taken from four depths (0.125, 0.325, 0.55 and 0.85 m) at five sites located at (0, 0.4), (0.38, 0.2), (0.38, -0.2), (-0.38, -0.2) and (-0.38, 0.2) m relative to each borehole.

The AT sorption isotherms were determined in triplicate for each sample with ^{14}C-ring-labelled molecules, basically following the recommendations of OECD Guideline 106 (Organization for Economic Co-operation and Development, 1981), with a 72-h contact time between the solids (5 g dry weight) and the $CaCl_2$ 10^{-2} solution with the

pesticide (10 ml). The working concentrations in the liquid phase ranged from 1 to 1000 $\mu g \, l^{-1}$ and were measured by liquid scintillation counting. The concentration bound to the solid was calculated as the difference between the concentrations in solution samples with and without solid. Typically, the precision of the mean K_f values were in the 5–10% range. More details of the procedures and the measurement errors can be found in Moreau and Mouvet (1997).

For the samples taken around the boreholes, the grain-size distribution and cation exchange capacity (CEC) were analysed following the AFNOR standard methods X31-107 and X31-130, respectively (AFNOR, 1983, 1985); the organic carbon content (OC) was measured by dry combustion at high temperature under an oxygen stream and the CO_2 produced was measured by infrared spectrometry (CS 125, Leco). For the samples taken in the three boreholes, the particle-size distribution was determined with the LABEX L-8903-11-2 standard method (LABEX methods, 1989), the OC with the Walkley and Black method (Nelson and Sommers, 1982) and the CEC using the LABEX L-8703-21-11 standard method (Ammonium acetate at pH 7, LABEX methods, 1987).

The measured AT adsorption isotherm was described with the Freundlich isotherm:

$$\frac{x}{m} = K_f C_e^n \tag{1}$$

where x/m (g kg^{-1}) is the concentration bound to the solid, C_e (g l^{-1}) is the concentration in solution at the end of the 72-h contact period, K_f and n are empirical constants. Parameters of Eq. (1) were obtained by fitting a straight line to the log-transformed concentration data (Fetter, 1993). For the (geo)statistical analyses in this study, K_f was raised to the power $1/n$ to obtain the same units for all estimated K_f-values, the n values being sometimes quite different from unity.

2.2. Stationarity assumptions and model building

A measured soil property, denoted by $z(x)$ where x is the vector containing the spatial coordinates and $x \in D$ (D being a subset of $\Re^3$), is assumed to be a realization of a stochastic random space function (RSF) $Z(x)$. $Z(x)$ is a continuous variable in space. The statistical properties of the RSF are determined based on the geostatistical model of regionalized variables (Matheron, 1963; Cressie, 1993). In this paper, we assume stationarity for the increments only, i.e., the intrinsic hypothesis. Taking the vector $h = x_1 - x_2$ as the lag distance between the two random variables $Z(x_1)$ and $Z(x_2)$, then this hypothesis is expressed as:

$$E[Z(x+h) - Z(x)] = 0 \tag{2}$$

and

$$E\left[(Z(x+h) - Z(x))^2\right] = 2\gamma(h) \tag{3}$$

where $\gamma(h)$ is the semivariogram. Together with the ergodicity assumption (Cressie, 1993), the intrinsic hypothesis is used in this paper to infer the statistical properties of the RSF.

In general, soil properties exhibit non-stationarity in both mean and variance (Hamlett et al., 1986), thus violating the assumptions made in the intrinsic hypothesis. Prior to

semivariogram estimation and modelling, a robust-resistant exploratory data analysis is performed using techniques described by Hamlett et al. (1986), Cressie and Horton (1987), Mohanty et al. (1991), Mohanty and Kanwar (1994) and Jacques et al. (1997). To handle non-stationarity of the mean, $Z(\boldsymbol{x})$ is decomposed into:

$$Z(\boldsymbol{x}) = \mu(\boldsymbol{x}) + \varepsilon(\boldsymbol{x}) \tag{4}$$

where $\mu(\boldsymbol{x})$ is the deterministic trend and $\varepsilon(\boldsymbol{x})$ is the stochastic small-scale variation with zero mean. The $\varepsilon(\boldsymbol{x})$ is characterized by a covariance function or semivariogram. The approach is now to estimate $\varepsilon(\boldsymbol{x})$ from the realization $z(\boldsymbol{x})$ by subtracting an estimate of $\mu(\boldsymbol{x})$ from $z(\boldsymbol{x})$. In a three-dimensional context, $Z(\boldsymbol{x})$ can be written as (Mohanty and Kanwar, 1994):

$$Z(x_1, x_2 \, x_3) = \mu + \delta_i(x_3) + \eta_j(x_1, x_2) + \sum_{u=1}^{2} \sum_{v=u+1}^{3} g_{uv}(x_u - \overline{x_u})(x_v - \overline{x_v})$$
$$+ \varepsilon(x_1, x_2, x_3) \tag{5}$$

where μ is the overall mean independent of location $\boldsymbol{x}$, δ_i is the depth effect ($i = 1, \ldots I$, with I number of vertical components), η_j the horizontal effect ($j = 1, \ldots, J$, with J number of locations in the horizontal plane where samples were taken), g_{uv} is a diagonal drift parameter in the $x_u - x_v$ plane and $\bar{x}_u$ are the averages of the individual x_u. The first three terms in Eq. (5) describe the additive effects, while nonadditive effects and interactions between horizontal and vertical effects are described with the fourth term in Eq. (5) (Cressie, 1993, p. 190; Mohanty and Kanwar, 1994). Estimations of the first three components of model (5) (μ, δ_i and η_j) were done using a resistant median polish algorithm described in detail by Cressie (1993) (p. 186). Median polish algorithms were found to be more robust with respect to outliers than mean polish algorithms (Cressie and Glonek, 1984; Mohanty et al., 1991). The estimated components, m, d_i and h_j of μ, δ_i and η_j, respectively, are subtracted from the measured value, $z(\boldsymbol{x})$. In a second step, the occurrence of diagonal trends and the significance of the drift parameters are explored. The values $(z(\boldsymbol{x}) - m - d_i - h_j)$ are plotted against $(x_u - \bar{x}_u)(x_v - \bar{x}_v)$. These plot are visually checked for trends and g_{uv} was fitted by linear regression. Finally, the estimated deterministic trend was subtracted from the measured $z(\boldsymbol{x})$ to obtain the residual $r(\boldsymbol{x})$, an estimate of $\varepsilon(\boldsymbol{x})$. Stationarity of variance was investigated using median–interquantile range squared (IQ^2) plots and, if necessary, a $\log_e$-transformation was used to stabilize the variance. After checking the stationarity in the mean and the variance, residuals were used in the geostatistical analysis.

2.3. Variogram estimation and model fitting

The semivariogram estimator, $\hat{\gamma}_z(\boldsymbol{h})$, as proposed by Matheron (1963) is given as:

$$\hat{\gamma}_z(\boldsymbol{h}) = \frac{1}{2N(\boldsymbol{h})} \sum_{i=1}^{N(\boldsymbol{h})} \left[r(\boldsymbol{x}_i + \boldsymbol{h}) - r(\boldsymbol{x}_i) \right]^2 \tag{6}$$

where $\boldsymbol{h}$ is the lag distance and $N(\boldsymbol{h})$ is the number of pairs separated by the lag

distance. The cross-semivariogram between the residuals of $z_1(\boldsymbol{x})$ and $z_2(\boldsymbol{x})$ is defined as:

$$\hat{\gamma}_{12}(\boldsymbol{h}) = \frac{1}{2N(\boldsymbol{h})} \sum_{i=1}^{N(\boldsymbol{h})} \left[r_1(\boldsymbol{x}+\boldsymbol{h}) - r_1(\boldsymbol{x}) \right] \left[r_2(\boldsymbol{x}+\boldsymbol{h}) - r_2(\boldsymbol{x}) \right] \qquad (7)$$

where $r_1(\boldsymbol{x})$ and $r_2(\boldsymbol{x})$ are the residuals of the random variables $z_1(\boldsymbol{x})$ and $z_2(\boldsymbol{x})$, respectively. This definition of the cross-semivariogram has the property that it is an even function symmetric in $(1, 2)$ $(\gamma_{12}(\boldsymbol{h}) = \gamma_{21}(\boldsymbol{h}))$ and in $(\boldsymbol{h}, -\boldsymbol{h})$ $(\gamma_{12}(\boldsymbol{h}) = \gamma_{12}(-\boldsymbol{h}))$. This implies the assumption of a symmetric cross-covariance function when the cross-semivariogram is used in the cokriging system (Journal and Huijbregts, 1978). However, the cross-covariance function is not by definition a symmetric function, due to a possible delay effect of a general lag of one variable behind the other (for a discussion, see Wackernagel, 1995; Goovaerts, 1997). When the delay effect is absent, the cross-variogram and the cross-semivariogram are equivalent tools. For the dataset considered in this paper, it is not likely to expect a delay effect between the different variables. An alternative is to use the so-called pseudo-cross-semivariogram as defined by Cressie (1993). However, two major disadvantages are linked to this pseudo-cross-semivariogram: (1) it makes only sense to use the pseudo-cross-semivariogram for variables with the same units representing the same phenomena, and (2) the pseudo-cross-semivariogram fails to express negative correlations between the variables. Given these constrains and given the specific objectives of this study, the cross-semivariogram defined in Eq. (7) is a valuable tool. The variograms and cross-variograms are calculated using the GSLIB software (Deutsch and Journel, 1992).

The experimental semivariograms are modelled using the spherical, exponential and Gaussian models (Webster, 1985; McBratney and Webster, 1986). These three different models are used since they differ in their shape near the origin and the estimated correlation length may differ between the different models. The spherical model is defined by three parameters: (i) C_0, the nugget variance which represents (a) the spatial variability at distances smaller than the sampling interval, (b) the variability within the sampling volume, and (c) the variability resulting from experimental errors, (ii) C_s, the structural variance, and (iii) a, the range. The exponential and Gaussian models are also described by C_0 and C_s, and by r, a parameter controlling the spatial range of the model.

An optimal set of parameters for each model is obtained by optimizing three validation criteria of the jackknife procedure which estimates the value at a location $\boldsymbol{x}_i$ based on the $N-1$ remaining observations using kriging (Vauclin et al., 1983). The three validation criteria are: (i) the kriged averaged error (KAE) with an optimal value of 0, (ii) the kriged reduced mean squared error (KRMSE) with an optimal value of 1, and (iii) the kriged mean squared error (KMSE) with an optimal value of 0 (Springer and Cundy, 1987; Russo and Jury, 1987a; Mohanty et al., 1991; Mallants et al., 1996, among others).

2.4. Spatial correlation analysis

A major drawback of the correlation coefficient, ρ_{XY}, is that it neglects the spatial location of the sample points. In order to account for the spatial location of the samples

and to study the correlation between the variables at different spatial scales, the codispersion coefficient, $\rho_{XY}(\boldsymbol{h})$, is used in the geostatistical analysis and is defined as:

$$\rho_{XY}(\boldsymbol{h}) = \frac{\gamma_{XY}(\boldsymbol{h})}{\sqrt{\gamma_{XX}(\boldsymbol{h})\gamma_{YY}(\boldsymbol{h})}} \tag{8}$$

where $\gamma_{XX}(\boldsymbol{h})$, $\gamma_{YY}(\boldsymbol{h})$, and $\gamma_{XY}(\boldsymbol{h})$ are, respectively, the semivariance of variable X and Y and the cross-semivariance between X and Y at lag distance $\boldsymbol{h}$. The codispersion coefficient expresses the correlation between the spatial increments of the random variables X and Y. In case of second-order stationarity, $\rho_{XY}(\boldsymbol{h})$ goes to ρ_{XY} for $|\boldsymbol{h}| \to \infty$ (Goovaerts, 1997). Plotting the codispersion coefficient as a function of $\boldsymbol{h}$ provides information about the correlation between two soil properties as a function of spatial scale (Goovaerts, 1997).

To summarize the correlation structure between all variables, the eigenvectors $\boldsymbol{\nu}$ of the codispersion matrices at lag distance $\boldsymbol{h}$, $\boldsymbol{P}(\boldsymbol{h}) = [\rho_{ij}(\boldsymbol{h})]$ with $i,j = 1, \ldots, p$ and p the number of variables, are calculated (i.e., principal component analysis; see Jobson, 1992). The correlation between the ith variable and the kth principal components of the codispersion matrices are calculated by multiplying the ith element of the kth eigenvector, $\boldsymbol{\nu}_{kj}$, by the square root of the eigenvalue of the kth eigenvector. This correlation between the variables and principal components, $\boldsymbol{\nu}_k *$ are then plotted in the space of the eigenvectors or principal components corresponding with the largest and the second largest eigenvalue of $\boldsymbol{P}(\boldsymbol{h})$. Thus, variable X_j is plotted at $(\boldsymbol{\nu}_{1j} *, \boldsymbol{\nu}_{2j} *)$ with $\boldsymbol{\nu}_{1j} *$ the jth element of the first eigenvector (corresponding to the largest eigenvalue) and $\boldsymbol{\nu}_{2j} *$ the jth element of the second eigenvector (corresponding to the second largest eigenvalue). Variables clustered together are correlated with each other. These so-called circle

Table 1
Statistical moments of non-transformed and $\log_e$-transformed variables

	Sand (%)	Loam (%)	Clay (%)	OC (%)	CEC (meq 100 g^{-1})	K_f (l kg^{-1})	n (−)	K_f^a (−)
Original variables								
Mean	28.7	54.2	16.4	0.71	9.555	1.17	0.92	1.25
Median	16.6	61.2	16.4	0.47	9.9	0.57	0.93	0.53
CV (%)	82.6	37.2	32.4	78.1	35.51	101.19	8.06	111.25
Max	90.4	72.8	30.5	2.4	16.8	4.8	1.09	6.33
Min	10.6	5.2	4.4	0.04	2.1	0.001	0.612	0.001
Log$_e$-transformed variables								
Mean	3.1	3.8	2.7	−0.7	2.2	−0.39	−0.09	−0.44
Median	2.8	4.1	2.80	−0.75	2.3	−0.56	−0.07	−0.64
CV (%)	21.1	17.4	14.2	−138.9	22.7	−145.0	−99.9	−180.1
Max	4.5	4.3	3.4	0.9	2.8	1.6	0.09	1.8
Min	2.4	1.6	−1.5	−3.2	0.74	−6.9	−0.49	−7.3

[a] K_f raised to the power $1/n$.

Table 2
Correlation matrix for the seven variables before applying the median polish algorithm

	Sand[a]	Loam	Clay	OC[a]	CEC[a]	Kf[ab]	n
Sand[a]	1						
Loam	−0.957[***]	1					
Clay	−0.545[***]	0.497[***]	1				
OC[a]	−0.735[***]	0.736[***]	0.129	1			
CEC[a]	−0.738[***]	0.771[***]	0.718[***]	0.44[***]	1		
K_f[ab]	−0.652[***]	0.677[***]	0.051	0.719[***]	0.351[***]	1	
n	−0.483[***]	0.549[***]	0.548[***]	0.264[**]	0.530[***]	0.104	1

[a]Log$_e$-transformed variable.
[***], [**], [*]: significantly different from 0 at a significancy level of 0.1%, 1%, and 5%, respectively (*P*-value < 0.001, 0.01 and 0.05, respectively).
[b]Raised to the power $1/n$.

of correlation allow comparison of the correlation structure between all variables at several lag distances *h*.

3. Results and discussion

Table 1 summarizes some descriptive statistics for the variables used in this study. Values were calculated using the 93 sample points and neglecting non-stationarity in the different directions. The largest variability was exhibited by K_f, followed by the sand content and the OC. The other variables have smaller coefficients of variation (CV). The correlation matrix is given in Table 2 and the circle of correlation of the first two principal components of the correlation matrix is plotted in Fig. 1. The sand content, OC, CEC and K_f were log$_e$-transformed to obtain the same units as those used in the geostatistical analysis (see next section). Also indicated in Fig. 1 is the percentage of the
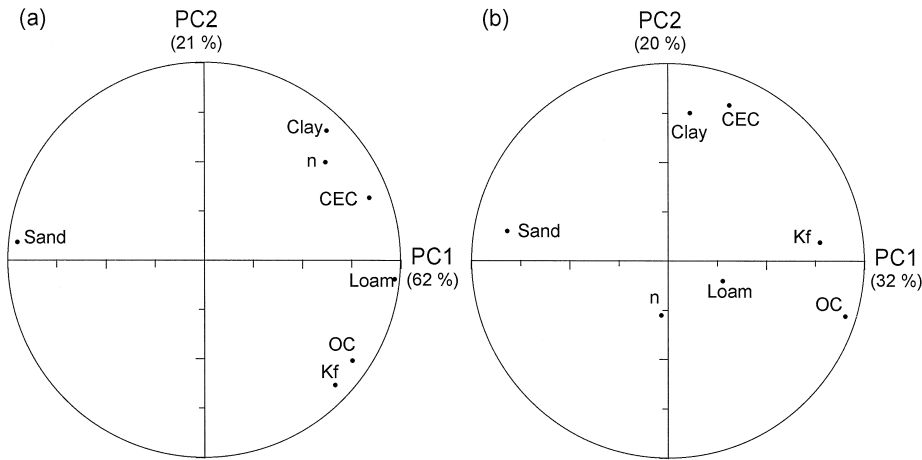

Fig. 1. Circle of correlation for the correlation matrix of (a) the original data, and (b) the median polished data.

total variance explained by the first or second eigenvector (Jobson, 1992). The K_f parameter was found positively correlated with the OC and the loam. Also, clay content, CEC and n parameter are found correlated with each other.

3.1. Analysis of data non-stationarity

For each of the seven variables, all observations used in this study are plotted against depth in Fig. 2. For better visualization of any trends in measured data, median values at seven layers were plotted. Most variables exhibit a nonlinear trend with depth. An abrupt change in sand content and loam content is observed at a depth of approximately 130 cm. Both the OC and K_f decrease sharply near the surface and remain constant with depth below 60 cm. The variation of n with depth is less pronounced. A small increase is observed at 50 cm depth for both the clay content and the CEC. The CEC also shows a sharp decrease between 100 and 150 cm depth. These observations indicate that the expected value of a soil property is dependent on the depth in the soil profile. Consequently, the depth factor has to be removed to carry out a meaningful geostatistical analysis.

The trend in the horizontal direction was investigated by estimating $E[Z(x+h) - Z(x)]$ (Eq. (2)) with (Vauclin et al., 1982; Berndtsson et al., 1993):

$$T(h) = \frac{1}{N(h)} \sum_{i=1}^{N(h)} [z(x_i + h) - z(x_i)] \tag{9}$$

where $h = (x_1, x_2, 0)$. Since $T(h)$ is the sample mean of the random variable $[z(x_i + h) - z(x_i)]$, it is approximately normally distributed by the law of large number and the central limit theorem. For independent identically distributed observations, $T(h)(N - 1)^{0.5}/S_{T(h)}$ should be between -1.96 and $+1.96$ if $T(h)$ is not statistically different from 0 at a significance level of 5%. In this test, we have that $S_{T(h)}$ is the standard deviation of $[z(x+h) - z(x)]$ and N is the number of observations. However, when $[z(x+h) - z(x)]$ are spatially dependent, the variance of $T(h)$ is:

$$\mathrm{Var}[T(h)]$$
$$= \frac{1}{N^2} \left[N\mathrm{Var}[U_h(x,h)] + \sum_i \sum_j \mathrm{Covar}[U_h(x_i,h)U_h(x_j,h)] \right] \quad i \neq j \tag{10}$$

where $U_h(x_i,h) = [z(x_i + h) - z(x_i)]$. Thus, in case of positively correlated $U_h(x_i,h)$, the variance of $T(h)$ will be underestimated if it is based on the variance of $[z(x+h) - z(x)]$. So, the estimated confidence intervals around $T(h)$ will be too narrow implying that the probability of rejecting the null hypothesis ($T(h) = 0$) is too high. Therefore, the proposed test should be interpreted as 'a worst-case scenario'. Furthermore, it is not our attempt to use this test in a strict statistical way, but rather as an exploratory tool to check the assumptions of stationarity. Therefore, we rather look at successive points of $T(h)$ as a function of h. To exclude the effect of depth, the values of each variable were transformed to an uniform score variable u ([0,1]) where $u = i/n_d$ with i the position in the ranked dataset $z^{(1)} < \ldots < z^{(n_d)}$ for each depth and n_d the number of observations at a specific depth. $T(h)$ was significantly different from zero
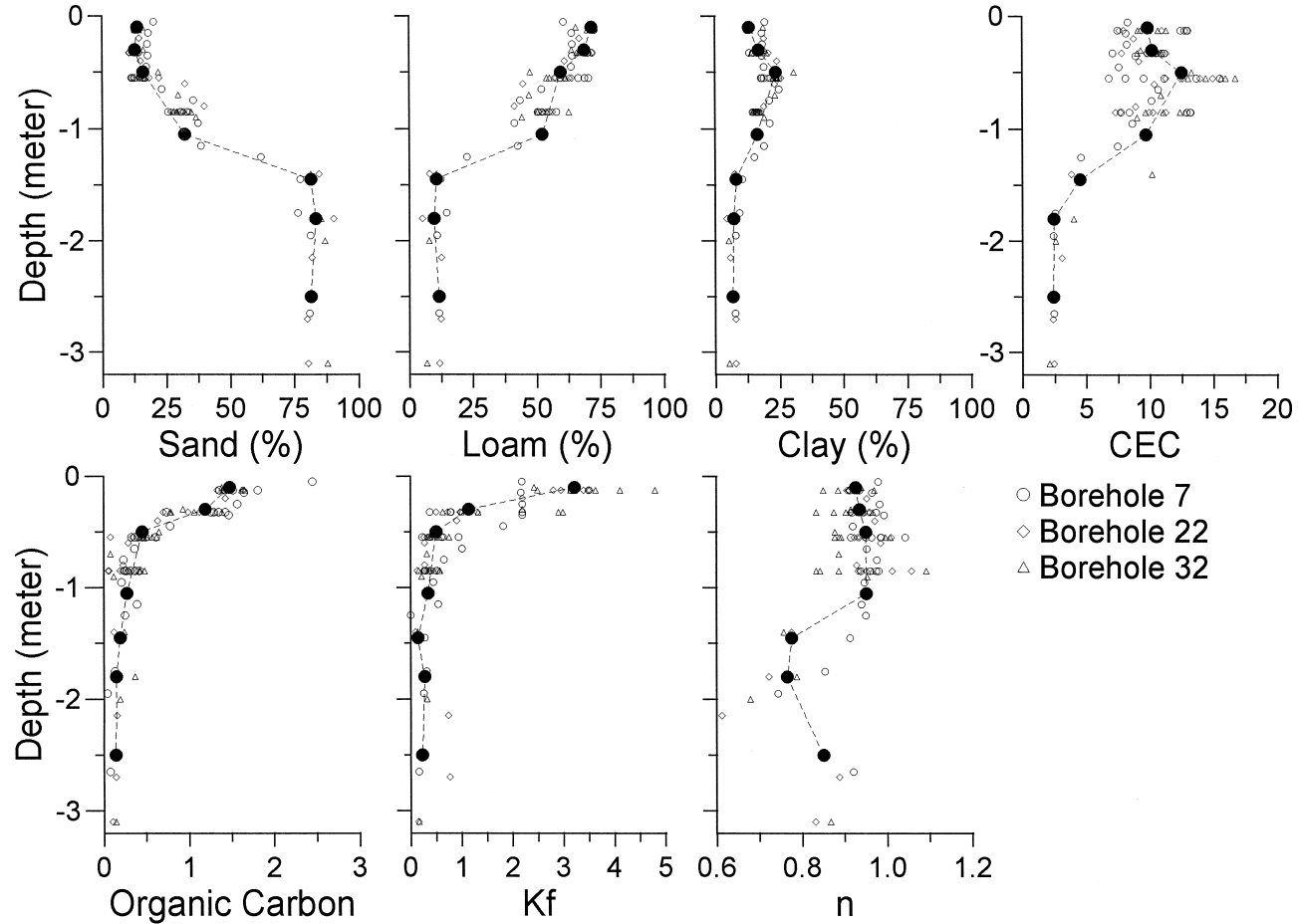
Fig. 2. Observed depth profiles of all variables for each borehole (open symbols) and medians for seven depths (solid circles).

for (i) OC and n at large lag distances ($h > 25$ m), and (ii) for sand, loam, clay and CEC for small lag distances ($h \approx 0.5$ m). $T(h)$ was not significantly different from zero for K_f (results not shown).

An in-depth analysis of the texture variables showed that the means of the boreholes are larger than the means in the surrounding clusters at the same depth. We suspect experimental artifact caused by different laboratories measuring texture and CEC. Consequently, to obtain an uniform dataset, the horizontal component of the trend was removed from all variables.

Different components of the large-scale variation were estimated with the median polish algorithm consisting of several iterations until convergence was met, i.e., m, d_i, and h_j do not change between two subsequent iterations. During the iteration procedure, normality and stationarity of variance were visually examined using histograms, probability plots, and median–IQ^2 plots. Log$_e$-transformed variables were used whenever necessary. Normality was checked by means of a quantile–quantile plot where the empirical quantiles are plotted versus the theoretical quantiles of the standard normal probability density function and these points are compared with a robust estimate of the expected relation (Chambers et al., 1983):

$$Q_r(p) = \text{Median} + \frac{\text{IQ}}{1.349} F^{-1}(p) \qquad (11)$$

where $Q_r(p)$ the theoretical reference line and $y = F^{-1}(p)$ is the inverse of the standard normal cumulative distribution function and $0 \leq p \leq 1$ ($p = F(y)$). To test if deviations
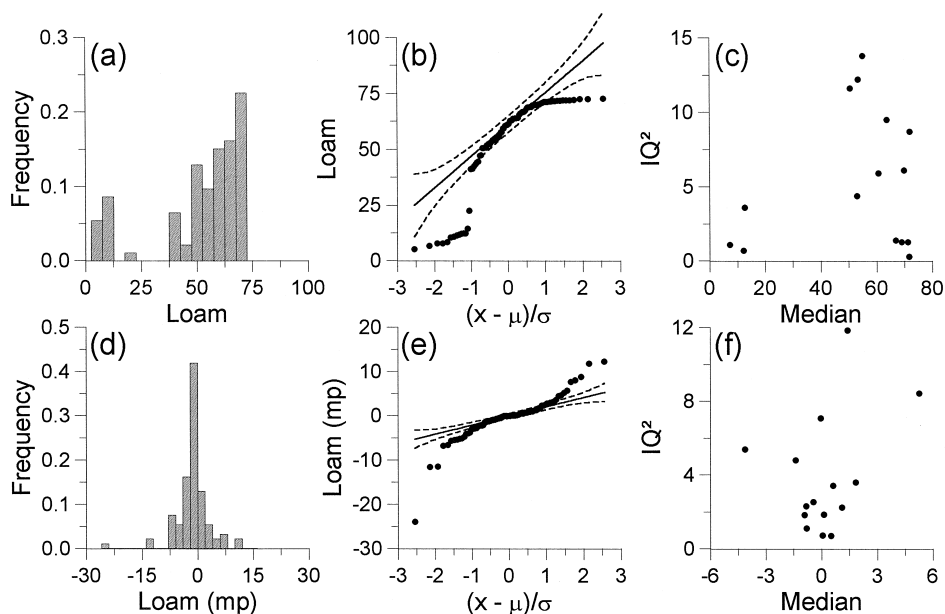

Fig. 3. Histogram (a,d), normal probability plot (b,e) and median–IQ^2-plot (c,f) of the observed loam content data (a,b,c) and the residuals after applying the median polish (mp) algorithm (d,e,f).

of the observation from $Q_r(p)$ were significant, a robust estimate of the 95% confidence intervals around $Q_r(p)$ were calculated as $[Q_r(p) \pm 1.96 \ s(p)]$ with $s(p)$ the standard error:

$$s(p) = \left[\frac{IQ}{1.349} \frac{1}{\exp(-0.5y^2)/\sqrt{2\pi}} \right] \left(\frac{p(1-p)}{N} \right)^{0.5} \tag{12}$$

where N the number of observations. Note that the estimation of the standard error is based on the assumption of independent identical distributed random observations.

In Figs. 3–5, the histogram, the normal probability plot with estimated confidence interval and the median–IQ^2 plot at different stages during the median polish algorithm
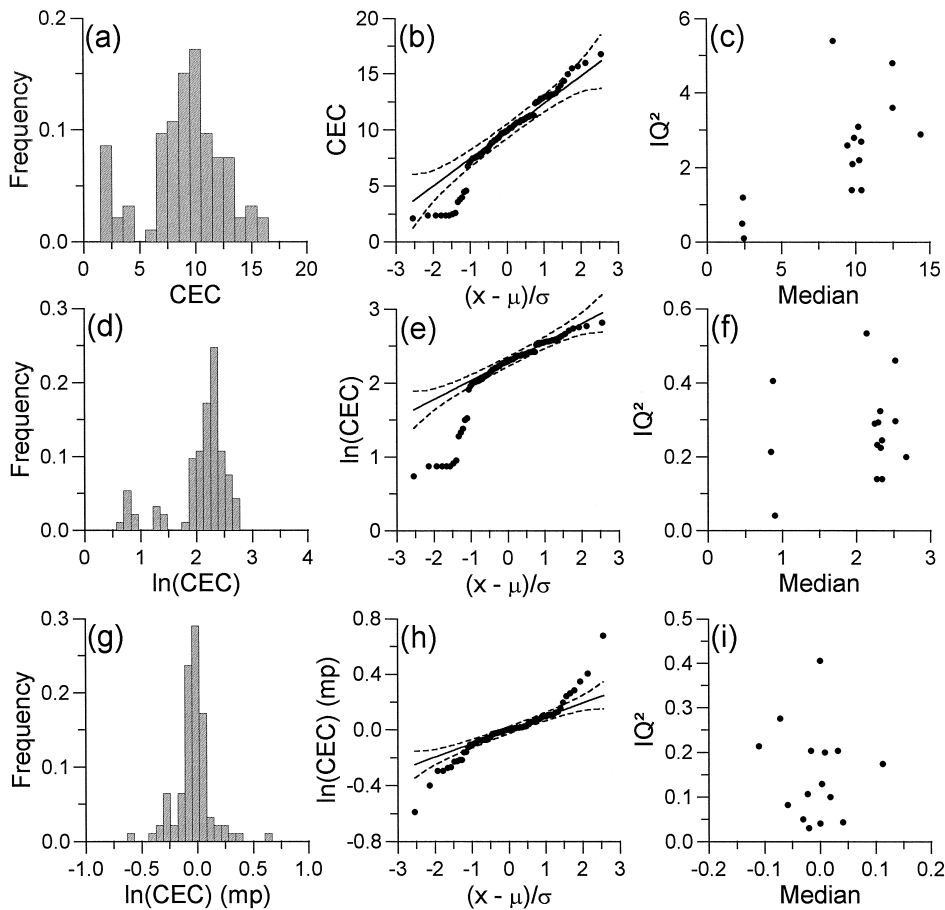

Fig. 4. Histogram (a,d,g), normal probability plot (b,e,h) and median–IQ^2-plot (c,f,i) of the observed CEC data (a,b,c), the $\log_e$-transformed data (d,e,f) and the residuals after applying the median polish (mp) algorithm (g,h,i).
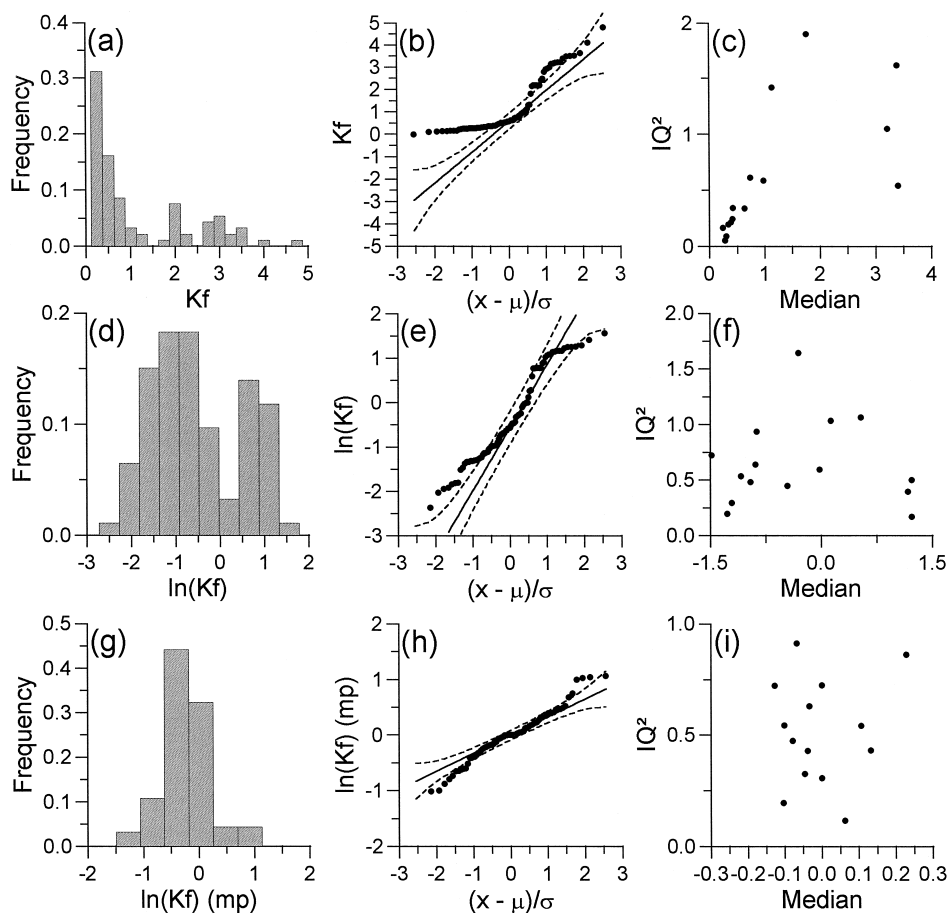
Fig. 5. Histogram (a,d,g), normal probability plot (b,e,h) and median–IQ^2-plot (c,f,i) of the observed K_f data (a,b,c), the log$_e$-transformed data (d,e,f) and the residuals after applying the median polish (mp) algorithm (g,h,i).

are given for the loam content, the CEC and the K_f, respectively. The median polish algorithm applied on the original data of the loam content, clay content and n provides a normally distributed residual data set showing stationarity in both mean and variance. For example, the original loam data shows a non-normal distribution (Fig. 3a,b) and non-stationarity in variance (Fig. 3c). After applying the median polish algorithm, the residuals are (i) normally distributed (as illustrated by the histogram [Fig. 3d] and the normal probability plot [Fig. 3e]), and (ii) stationary in variance (Fig. 3f). Similar results were obtained for the clay content and n. A log$_e$-transformation was required for the other four variables. For the CEC and the sand content, log$_e$-transformation resulted in a much stabilized variance (e.g., CEC-data, Fig. 4c vs. f). After applying the median polish algorithm, residuals exhibited constancy in median and followed a normal
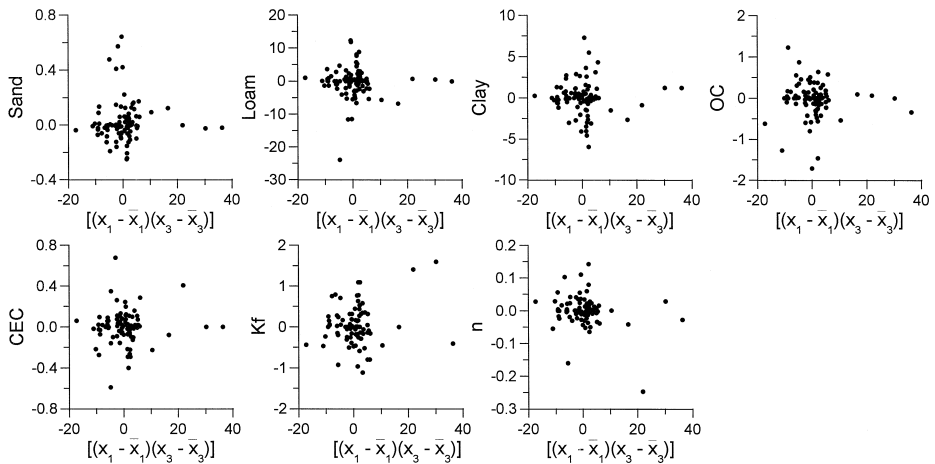
Fig. 6. Diagnostic plots to investigate the interaction effect in the $x_1 - x_3$ plane.

distribution (e.g., CEC-data, Fig. 4a,d vs. g, and Fig. 4b,e vs. h). The $\log_e$-transformation of OC and K_f resulted both in a more normally distributed data set (e.g., K_f-data, Fig. 5b vs. e) and stationarity in variance (e.g., K_f-data, Fig. 5c vs. f).

Subsequently, possible interactions between the horizontal and vertical effects were investigated in the $x_1 - x_2$, the $x_1 - x_3$ and the $x_2 - x_3$ planes. Fig. 6 shows the diagnostic plots for all variables in the $x_1 - x_3$ plane. No trends were observed for any of the variables. The estimated g_{13}-values are all smaller than 0.003 with a maximum R^2 of 0.05. Similar observations were made in the other two planes. Therefore, all g_{ij}'s in the model (Eq. (5)) were put equal to zero. For all variables, the median polish algorithm was successful in deriving a residual set which obeys the intrinsic hypothesis or the second order stationarity.

3.2. Variogram analysis

Vertical variograms were estimated at six lag distances, i.e., 0.17, 0.28, 0.5, 0.84, 1.36, and 2.03 m, using 30, 62, 54, 56, 32, and 27 data pairs, respectively. Fig. 7 presents estimated variogram and fitted models for different variables. Two groups of variograms can be distinguished. The sand, loam, clay and K_f variograms reveal pure nugget. The other three variograms (OC, CEC, n) showed a spatial structure. Different models (spherical, exponential and Gaussian) were used to describe these three variograms. As a consequence of the lack of points at both small and large lag distances, we cannot discriminate between the three models since they behave differently at these lag distances (McBratney and Webster, 1986). In addition, the estimates of the nugget, the sill and the correlation length (three parameters useful in stochastic modelling and sensitivity analysis of solute transport in heterogeneous field soils) may be different for the different models.
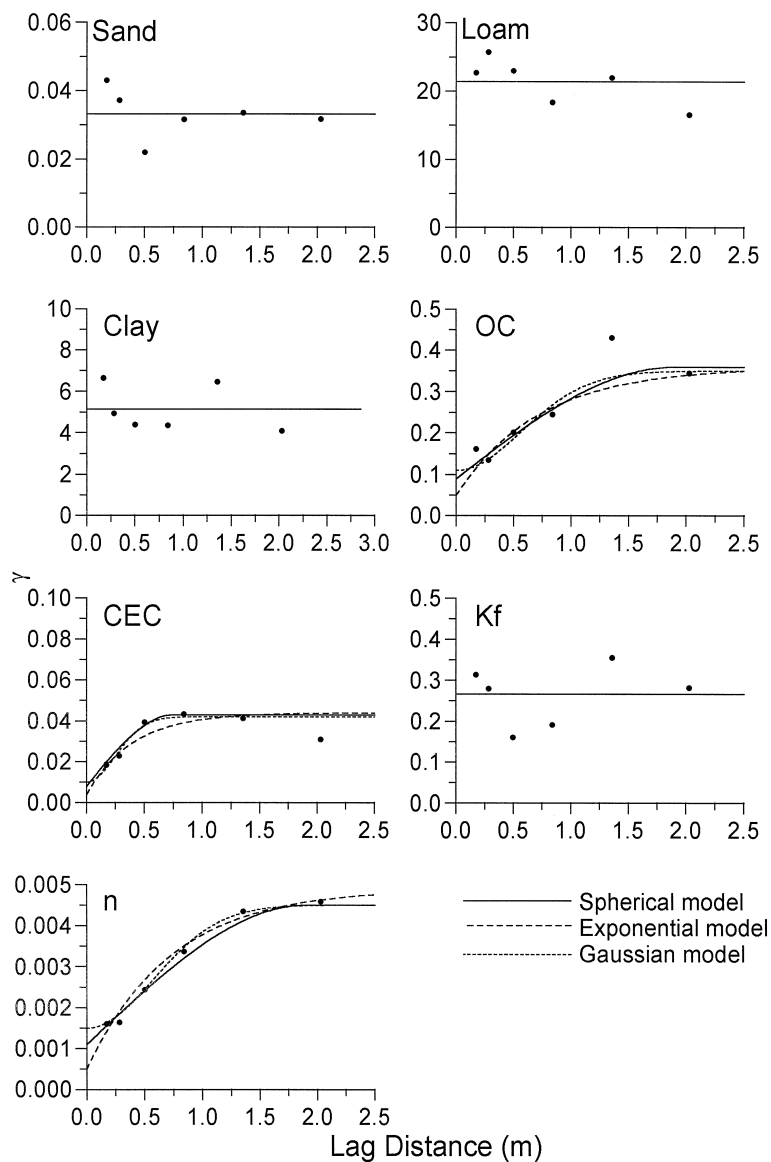
Fig. 7. Experimental vertical semivariograms of the residuals (solid circles). Decreasing dash lengths: fitted spherical, exponential and Gaussian variogram models.

The fitted model parameters and corresponding validation criteria are given in Table 3. The validation criteria are reasonably close to their optimal values. The three models describe the experimental variograms with approximately the same degree of accuracy. In general, $C_0 + C_s$ for the three models are quite close to each other, although C_0/C_s

Table 3
Estimated parameters and validation criteria for the spherical and exponential models

Variable	C_0	C_s	a (m)	I^* (m)	KAE	KMSE	KRMSE
Spherical model							
OC	0.0900	0.2700	1.90	0.63	−0.0034	0.4209	0.9530
CEC	0.0080	0.0340	0.75	0.25	−0.0022	0.1785	0.9936
n	0.0011	0.0034	1.90	0.63	−0.0013	0.0537	1.0545
Exponential model							
OC	0.0500	0.3100		0.73	−0.0048	0.4208	0.9793
CEC	0.0040	0.0400		0.40	−0.0016	0.1802	1.0486
n	0.0005	0.0044		0.73	−0.0019	0.0549	1.0839
Gaussian model							
OC	0.1100	0.2400		0.81	−0.0058	0.4184	0.9829
CEC	0.0100	0.0320		0.35	−0.0030	0.1779	1.0490
n	0.0015	0.0030		0.81	−0.0014	0.0554	1.0756

differs between the three models. The correlation length scale, I^* (Jury et al., 1991), also depends on the model used.

The contribution of the trend to the total observed variance is quantified as (Russo and Jury, 1987b; Russo and Bouton, 1992):

$$C_d = \sum_{k=1}^{N} \left[m(\boldsymbol{x}_k) - m \right]^2 / N = \sum_{k=1}^{N} \left[d_i(x_{3k}) + h_j(x_{1k}, x_{2k}) \right]^2 / N \qquad (13)$$

where $\boldsymbol{x}_k$ is the spatial coordinate of the kth sample and $m(\boldsymbol{x}_k) = m + d_i(x_{3k}) + h_j(x_{1k}, x_{2k})$. The other two components (C_0 and C_s) are obtained from the fitted model parameters. Estimates of the total variance and the percentage of each component in the total variance are given in Table 4.

Except for CEC, estimated variance is larger than or equal to the observed variance (Table 1). In the geostatistical analysis, we take into account the correlation between nearby samples resulting in this larger variance (Russo and Bouton, 1992). The contribution of the deterministic variation, C_d, was more than 85% for the four variables without spatial structure and for CEC. This again confirmed the non-stationarity in the data. A lower contribution of C_d was observed for the OC and n. The contribution of C_0 for all variables was low (sand, loam, OC and CEC) to moderate (clay, K_f and n). For the three variables with a spatial correlation structure (OC, CEC, n), C_s contributes considerably to the observed variance of the trend-free data.

3.3. Correlation analysis

The result of the classical correlation analysis is given in Table 2 and plotted in Fig. 1. The correlation between the original data was high and 19 correlation coefficients were found to be significantly different from 0 at a significance level of 0.1% (P-value

Table 4
Estimated variance based on the geostatistical analysis and the contribution of different components to the total variance

	Total variance	C_d (%)	C_0 (%)	C_s (%)
Pure nugget				
Sand	0.514	93.5	6.5	–
Loam	400.03	94.7	5.3	–
Clay	42.92	88.0	12.0	–
K_f	1.780	85.1	14.9	–
Spherical model				
OC	1.507	76.0	6.0	18.0
CEC	0.292	85.6	2.7	11.7
n	0.0078	42.3	14.1	43.6
Exponential model				
OC	1.507	76.0	3.3	20.7
CEC	0.294	85.0	1.4	13.6
n	0.0082	40.2	6.1	53.7
Gaussian Model				
OC	1.497	76.6	7.3	16.1
CEC	0.292	85.6	3.4	11
n	0.0078	42.3	19.1	38.6

< 0.001, Table 2). However, the classical analysis neglects the spatial location of the sample points and the trend with depth. In this section, the residuals and the cross-variograms are used to explore further the correlation coefficients between the variables at different spatial scales.

Correlation coefficients between the residuals were lower than the ones in Table 2 and only four correlation coefficients are significantly different from 0 at a significancy level of 0.1% (*P*-value < 0.001) and one at 1% (K_f-CEC) (*P*-value < 0.01). Negative correlation coefficients were found between sand and loam content (-0.75), and sand content and K_f (-0.37). The clay content and CEC (0.37), loam content and K_f (0.60) and CEC and K_f (0.31) were positively correlated. This indicates that the trend in the vertical direction has an important influence on the correlation coefficient between the soil properties. As a consequence, the first principal component of the residuals explains a smaller percentage of the total variance (only 32%, Fig. 1b).

The correlation between soil properties may depend on the spatial scale, as was shown by Goovaerts (1997). One way to express this relation is by defining a codispersion correlation coefficient (Eq. (8)): if the codispersion between the variables is constant for different lag distances, the correlation structure of the variables is not affected by spatial scale (Wackernagel, 1995). A positive codispersion correlation coefficient at a lag distance h means that an increase in one of the variables over a lag distance h corresponds with an increase in the other variable over the same lag distance. To calculate the codispersion correlation coefficients, the experimental cross-variograms between all variables were calculated in the vertical direction at the same six lag

distances (results not shown). Since the units are different between the variables, the residuals were standardized to zero mean and unit variance. Most of the experimental cross-variograms were irregular. These irregularities may be due to (i) poor spatial correlation of the variable(s), and (ii) small codispersion coefficients (Goovaerts, 1997).

To investigate the correlation between different variables, the principal components of the codispersion correlation matrix were calculated for each lag distance and the circle of correlation was constructed for each lag distance (Fig. 8). Apparently, the correlation structure between the variables changes considerably between different spatial increments h. This is probably due to the irregular experimental cross-variograms and relative small sample size used in this study. However, some interesting observations were made. An important observation is that K_f is positively correlated with OC at almost all spatial increments (except at $h = 0.5$). The codispersion correlation coefficient between K_f and OC ranges between 0.24 (at $h = 2.03$ and $h = 0.841$) and 0.44 ($h = 1.356$). Furthermore, variables appeared to be correlated with each other when the spatial location of the observation is accounted for. At the smallest lag distance ($h = 0.173$), we observe a strong correlation between clay content, CEC and n (Fig. 8a). At larger lag distances ($h = 0.283$ and $h = 0.5$), the correlation between clay content and CEC remains where n is no longer correlated with these two variables. In the largest two lag distances ($h = 2.03$), we observed no correlation between clay content and CEC, whereas n is strongly correlated with clay content ($\rho_{XY}(2.03) = 0.40$). In the classical correlation analysis (neglecting the spatial locations), no strong correlation was observed between median-polished residuals of the clay content and CEC on one side and n on the other side. Note that the correlation between clay content and n or between K_f and OC is present in the residuals.
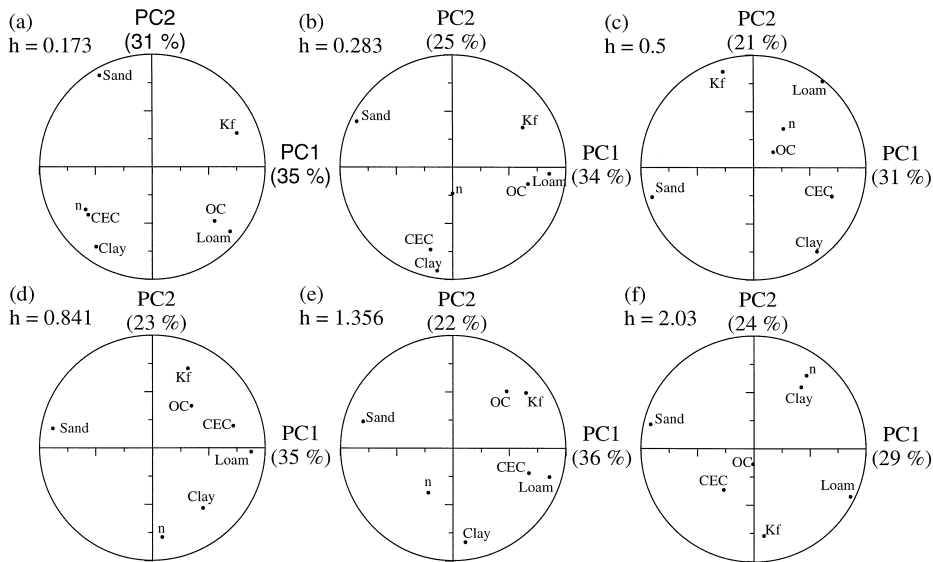

Fig. 8. Circle of correlation of the codispersion matrix at six spatial increments.

4. Conclusions

The spatial variability of the parameters of the Freundlich isotherm for atrazine has been characterized using the theory of regionalized variables. Given the trend with depth of all variables, the analysis required methods that can handle these non-stationary effects. The correlation of the sorption parameters with some physical (texture), chemical (CEC) and biological (OC) properties of soil has also been investigated.

A significant part of the observed variability of all soil properties results from deterministic variation in the vertical direction and, to a lesser extent, in the horizontal direction. We found that the large-scale variability was responsible for more than 85% of the observed variance for most variables. Removing the deterministic component results in residuals that correlate much less with each other than the original data. Therefore, the estimation of K_f and n from basic soil properties (such as texture, OC and CEC) should be restricted to the determination of large-scale deterministic variability (e.g., soil layers or different soil types). Due to the low correlation coefficients between the residuals of the basic soil properties and the residuals of the AT sorption parameters, it is not possible to obtain an exact picture of the actual small-scale heterogeneity of K_f and n using regression equations based on the measured basic soil properties in this study.

The experimental vertical semivariograms of the residuals of OC, CEC, and n showed a spatial correlation structure. The estimated correlation length scale depends on the variogram model and ranged between 0.25–0.40 m for CEC and 0.63–0.81 m for OC and n. The vertical variograms of the texture variables and K_f revealed pure nugget. The codispersion coefficients, which express the correlation between two variables over a spatial increment $\boldsymbol{h}$, change considerably between the different spatial increments.

The data on (i) the spatial correlation of atrazine sorption parameters and soil properties, and (ii) spatial correlation between soil properties such as presented in this study, will be useful in future stochastic analysis of solute transport in heterogeneous soils. Note that the study was performed using a limited data set and for one field site with a specific geological profile. Applicability of the statistical parameters to predict the behaviour of atrazine in other field plots is thus questionable. However, the presented statistics can be included in a databank containing distributions (cf. Table 1), correlations (cf. Table 2), correlation lengths for different variogram models (cf. Table 3) and contributions of different factors to the variance (cf. Table 4) of soil properties related to reactive contaminant transport for a range of different soil types. The results of this and other similar studies (i.e., the statistical parameters of the multivariate probability density function and the covariance functions of the atrazine adsorption parameters) can be used in theoretical studies based on unconditional Monte-Carlo simulations of reactive transport under (un)saturated steady-state/transient flow conditions in spatially correlated heterogeneous multidimensional random fields. Such theoretical studies may contribute to our understanding of factors influencing the plume movement in soils with variable properties. In this way, the relation between the observed variability of local-scale adsorption parameters and the effective field-scale transport parameters describing the retardation and the dispersion of a reactive solute plume can be

investigated and quantified similar to studies with variability of soil hydraulic properties (e.g., Roth and Hammel, 1996; Vanderborght et al., 1997).

References

AFNOR, 1983. Soils quality. Particle size determination by sedimentation. Pipette method. AFNOR X31 107, July 1983, 15 pp.

AFNOR, 1985. Soils quality. Determination of exchange capacity and exchangeable cations. AFNOR X31 130, June 1985, 14 pp.

Beck, A.J., Harris, G.L., Howse, K.R., Johnson, A.E., Jones, K.C., 1996. Spatial and temporal variation of isoproturon residues and associated sorption/desorption parameters at the field scale. Chemosphere 33, 1283–1295.

Berndtsson, R., Bahri, A., Jinno, K., 1993. Spatial dependence of geochemical elements in a semiarid agricultural field: II. Geostatistical properties. Soil Sci. Soc. Am. J. 57, 1323–1329.

Bellin, A., Rinaldo, A., 1995. Analytical solutions for transport of linearly adsorbing solutes in heterogeneous formations. Water Resour. Res. 31, 1505–1511.

Brusseau, M.L., Jessup, R.E., Rao, P.S.C., 1989. Modeling the transport of solutes influenced by multiprocess nonequilibrium. Water Resour. Res. 25, 1971–1988.

Chambers, J.M., Cleveland, W.S., Kleiner, B., Tukey, P.A., 1983. Graphical Methods for Data Analysis. Wadsworth Publishing, Belmont, CA.

Cressie, N.A.C, 1993. Statistics for Spatial Data. Wiley, NY, 900 pp.

Cressie, N.A.C., Glonek, F., 1984. Median-based covariogram estimators reduce bias. Stat. Probab. Lett. 2, 299–304.

Cressie, N.A.C., Horton, R., 1987. A robust-resistant spatial analysis of soil water infiltration. Water Resour. Res. 23, 911–917.

Deutsch, C.V., Journel, A.G., 1992. GSLIB, Geostatistical Software Library and User's Guide. Oxford University Press, NY, 340 pp.

Driessen, P.M., Dudal, R., 1991. Lectures notes on the geography, formation, properties and use of the major soils of the world. Agricultural University Wageningen and K.U. Leuven.

Fetter, 1993. Reference Contaminant Hydrology, Maxwell Macmillan, 458 pp.

Flury, M., 1996. Experimental evidence of transport of pesticides through field soils—a review. J. Environ. Qual. 25, 25–45.

Flury, M., Leuenberger, J., Studer, B., Flühler, H., 1995. Transport of anions and herbicides in a loamy and a sandy field soil. Water Resour. Res. 30, 1945–1954.

Goovaerts, P., 1992. Geostatistics for Natural Resource Evaluation. Oxford University Press, NY, 483 pp.

Hamlett, J.M., Horton, R., Cressie, N.A.C., 1986. Resistant and exploratory techniques for use in semivariogram analysis. Soil Sci. Soc. Am. J. 50, 868–875.

Jacques, D., Vanderborght, J., Mallants, D., Mohanty, B.P., Feyen, J., 1997. Analysis of solute redistribution in heterogeneous soil: 1. Geostatistical approach to describe the spatial scaling factors. In: Soares, A., et al. (Eds.), geoENV I—Geostatistics for Environmental Applications. Kluwer Academic Publishers, 271–282.

Jobson, J.D., 1992. Applied multivariate data analysis. Volume II: Categorical and Multivariate Methods. Springer-Verlag, NY, 731 pp.

Journal, A., Huijbregts, C., 1978. Mining Geostatistics. Academic Press, NY.

Jury, W.A., Gruber, J., 1989. A stochastic analysis of the influence of soil and climatic variability on the estimate of pesticide groundwater pollution potential. Water Resour. Res. 25, 2465–2474.

Jury, W.A, Gardner, W.R., Gardner, W.H., 1991. Soil Physics, 5th edn. Wiley, New York, 300 pp.

Kladivko, E.J., van Scoyoc, G.E., Monke, E.J., Oates, K.M., Pask, W., 1991. Pesticide and nutrient movement into subsurface tile drains on a silt loam soil in Indiana. J. Environ. Qual. 20, 264–270.

LABEX methods, 1987. L-8703-21-11. Cation Exchange Capacity.

LABEX methods, 1989. L-8903-11-2. Particle size analysis (pipette).

Ma, L., Selim, H.M., 1994. Predicting the transport of atrazine in soils: second-order and multireaction approaches. Water Resour. Res. 30, 3489–3498.

Mallants, D., Mohanty, B.P., Jacques, D., Feyen, J., 1996. Spatial variability of hydraulic properties in a multi-layered soil profile. Soil Sci. 161, 167–181.

Matheron, G., 1963. Principles of geostatistics. Econ. Geol. 19, 129–149.

McBratney, A.B., Webster, R., 1986. Choosing functions for semi-variogram of soil properties and fitting them to sampling estimates. J. Soil Sci. 37, 617–639.

Mohanty, B.P., Kanwar, R.S., 1994. Spatial variability of residual nitrate–nitrogen under two tillage systems in central Iowa: a composite three-dimensional resistant and exploratory approach. Water Resour. Res. 30, 237–251.

Mohanty, B.P., Kanwar, R.S., Horton, R., 1991. A robust-resistant approach to interpret spatial behavior of saturated hydraulic conductivity of a glacial till soil under no-tillage system. Water Resour. Res. 27, 2979–2992.

Moreau, C., Mouvet, C., 1997. Sorption and desorption of atrazine, deethylatrazine and hydroxyatrazine by soil and aquifer solids. J. Environ. Qual. 26, 416–424.

Nelson, D.W., Sommers, L.E., 1982. Total carbon, organic carbon, and organic matter. In: Page, A.L., Miller, R.H., Keeney, D.R. (Eds.) Methods of soil analysis, Part 2—Chemical and Microbiological Properties, 2nd edn. Agronomy Monograph, no. 9, ASA-SSSA, Madison, WI, USA, 539–594.

Organization for Economic Co-operation and Development, 1981. Guidelines for testing of chemicals. Guideline 106: Sorption/Desorption. Paris, France, May 1981, 24 pp.

Roth, K., Hammel, K., 1996. Transport of conservative chemical through an unsaturated two-dimensional Miller-similar medium with steady state flow. Water Resour. Res. 32, 1653–1663.

Russo, D., Bouton, M., 1992. Statistical analysis of spatial variability in unsaturated flow parameters. Water Resour. Res. 28, 1911–1925.

Russo, D., Jury, W.A., 1987a. A theoretical study of the estimation of the correlation scale in spatially variable fields: 1. Stationary fields. Water Resour. Res. 23, 1257–1268.

Russo, D., Jury, W.A., 1987b. A theoretical study of the estimation of the correlation scale in spatially variable fields: 2. Nonstationary fields. Water Resour. Res. 23, 1269–1279.

Springer, E.P., Cundy, T.W., 1987. Field-scale evaluation of infiltration parameters from soil texture for hydrologic analysis. Water Resour. Res. 23, 325–333.

Traub-Eberhard, U., Henschel, K.-P., Kördel, W., Klein, W., 1995. Influence of different field sites on pesticide movement into subsurface drains. Pest. Sci. 43, 121–129.

Tseng, P.-H., Jury, W.A., 1994. Comparison of transfer function and deterministic modeling of area-averaged solute transport in a heterogeneous field. Water Resour. Res. 30, 2051–2063.

Vanderborght, J., Jacques, D., Mallants, D., Tseng, P.-H., Feyen, J., 1997. Comparison between field measurements and numerical simulation of steady-state solute transport in a heterogeneous soil profile. Hydrol. Earth System Sci. 1, 853–871.

van der Zee, S.E.A.T.M., Boesten, J.J.T.I., 1991. Effects of soil heterogeneity on pesticide leaching to groundwater. Water Resour. Res. 27, 3051–3063.

Vauclin, M., Vieira, S.R., Bernard, R., Hatfield, J.L., 1982. Spatial variability of surface temperature along two transects of a bare soil. Water Resour. Res. 18, 1677–1686.

Vauclin, M., Vieira, S.R., Vachaud, G., Nielsen, D.R., 1983. The use of co-kriging with limited field soil observations. Soil Sci. Soc. Am. J. 47, 175–184.

Vereecken, H., Jaekel, U., Mouvet, C., Moreau, C., Bureaul, P., Dust, M., Kim, D.-J., Jacques, D., Feyen, J., Georgescu, J., Suciu, A., Marinoschi, N.G., 1996. Critical parameters governing the mobility and fate of pesticides in soil-aquifer systems. In: Del Re, A.M., Capri, E., Evans, S.P., Trevisan, M. (Eds.), The Environmental Fate of Xenobiotics, Proceedings of the Xth Symposium of Pesticide Chemistry, Sept. 30–Oct. 2, Piancenza, Italy, pp. 627–648.

Wackernagel, H., 1995. Multivariate Geostatistics. Springer-Verlag, Berlin, 255 pp.

Webster, R., 1985. Quantitative spatial analysis of soil in the field. Adv. Soil Sci. 3, 1–70.

Yang, J., Zhang, R., Wu, J., 1996a. An analytical solution of macrodispersivity for adsorbing solute transport in unsaturated soils. Water Resour. Res. 32, 355–362.

Yang, J., Zhang, R., Wu, J., Allen, M.B., 1996b. Stochastic analysis of adsorbing solute transport in two-dimensional unsaturated soils. Water Resour. Res. 32, 2747–2756.